Int. J. Electrochem. Sci., 8 **(2013)** 2504 - 2514

International Journal of
ELECTROCHEMICAL
SCIENCE
www.electrochemsci.org

Preparation and Electrochemical Properties of Nanometer-Sized Li_2TiO_3-$LiCrO_2$ Nanocomposite Cathode Powders by Spray Pyrolysis

You Na Ko[1], *Yun Chan Kang*[1,*], *Seung Bin Park*[2]

[1] Department of Chemical Engineering, Konkuk University, 1 Hwayang-dong, Gwangjin-gu, Seoul 143-701, Korea
[2] Department of Chemical and Biomolecular Engineering, Korea Advanced Institute of Science and Technology, 291 Daehak-ro, Yuseong-gu, Daejeon 305-701, Korea
[*]E-mail: yckang@konkuk.ac.kr

Received: 5 November 2012 / *Accepted:* 25 November 2012 / *Published:* 1 February 2013

The nanometer-sized Li_2TiO_3-$LiCrO_2$ nanocomposite cathode powders are prepared by spray pyrolysis. The existence of Li_2CrO_4 glass material during post-treatment is essential to prepare the nanometer-sized Li_2TiO_3-$LiCrO_2$ nanocomposite powders. The Li_2TiO_3-$LiCrO_2$ nanocomposite powders washed with distilled water have the mixed crystal structure of the rhombohedral $LiCrO_2$ and the monoclinic Li_2TiO_3 without impurity. The mean size of the nanocomposite powders post-treated at 750°C is 130 nm. The initial charge and discharge capacities of the nanocomposite powders post-treated at 750°C are 303 and 195 mAh g^{-1}, respectively. The capacity retention of the nanocomposite powders post-treated at 750°C is 88% after 30 cycles.

Keywords: nanocomposite, spray pyrolysis, composite powders, cathode powders

1. INTRODUCTION

Layered lithium manganese oxides have been widely investigated as cathodes for lithium secondary batteries due to their low toxicity and low cost. However, the practical application of $LiMnO_2$ is restricted by the transformation into a spinel structure during cycling [1,2].

Recently, layered cathode materials based on the Li_2MnO_3-$LiMO_2$ (M = Cr, Ni, Co, or Fe) composite have been attracting much attention due to the improved electrochemical properties of the cathode materials [3-13]. Among the solid solutions, Cr-based cathode materials (Li_2MnO_3-$LiCrO_2$)

were attracting much interest because of the high capacity and stable cycleability which results from the three-electron redox couple of Cr^{3+}/Cr^{6+}, instead of Mn [14-18]. In the layered Li_2MnO_3-$LiCrO_2$ composite, Mn is maintained in the 4^+ oxidation state which maintains the structural stability of the cathode materials [18].

Li_2TiO_3, which is an isostructural component with Li_2MnO_3 and has a strong Ti-O bond relative to Mn-O, can remarkably stabilize the layered $LiMO_2$ cathode components. Thus, application of the Li_2TiO_3 for layered $LiMO_2$ cathode material has been attempted instead of the Li_2MnO_3 [19-22]. However, synthesis of the Li_2TiO_3-$LiCrO_2$ was not attempted by gas-phase reaction, and only studied by some solid-state reaction and liquid solution methods [22-24]. Zhang et al. [23] synthesized the layered Li-Cr-Ti-O cathode materials related to the Li_2TiO_3-$LiCrO_2$ solid solution by conventional solid-state reaction. The sample with [Li/(Cr+Ti)] = 1.5 showed an initial discharge capacity of 152 mAh g^{-1} between 2.0 and 4.8 V at a constant density of 32 mA g^{-1}. Mi et al. [24] reported the synthesis of the carbon-coated $Li[Cr_xLi_{(1/3-x/3)}Ti_{(2/3-2x/3)}]O_2 (0.3 \leq x \leq 0.45)$ by a sol-gel method. The sample of $x = 0.4$ showed the high initial discharge capacity of 207 mAh g^{-1} between 2.5 and 4.4 V at a constant current density of 30 mA g^{-1}.

Spray pyrolysis, which is one of the gas-phase reaction methods, is proper for the preparation of multicomponent cathode materials due to the simple control of the composition of the cathode materials [25-28]. In this study, Li_2TiO_3-$LiCrO_2$ nanocomposite cathode powders were prepared by spray pyrolysis. The physical and electrochemical properties of the Li_2TiO_3-$LiCrO_2$ nanocomposite cathode powders post-treated at various temperatures were investigated. Due to the generation of the Li_2CrO_4 impurity phase and the removal of impurities by washing, nanometer-sized Li_2TiO_3-$LiCrO_2$ nanocomposite cathode powders were formed.

2. EXPERIMENTAL

The 0.55 Li_2TiO_3-0.45 $LiCrO_2$ (equivalently $Li_{1.216}Cr_{0.353}Ti_{0.431}O_2$) composite cathode powders were prepared by spray pyrolysis. The equipment consisted of six ultrasonic spray generators operating at 1.7 MHz, a quartz reactor, and a bag filter. The starting materials were lithium nitrate, chromium nitrate nonahydrate, and titanium tetra-iso-propoxide (TTIP). A small amount of nitric acid was used to peptize the hydrolyzed TTIP and form a clear solution. The concentration of metal components was fixed at 0.5 M, and the lithium component in excess of 5% weight of the stoichiometric amount was added to a spray solution. The preparation temperature and the flow rate of air used as the carrier gas were fixed at 1000^oC and 10 $Lmin^{-1}$, respectively. The precursor powders prepared by spray pyrolysis were post-treated at various temperatures for 12 h in an air atmosphere. The post-treated powders were washed in distilled water to remove the Li_2CrO_4 impurity and dried at 120^oC.

The morphologies of the precursor and post-treated cathode powders before and after washing were investigated by scanning electron microscopy (SEM, JEOL JSM-6060) and transmission electron microscopy (TEM, JEOL JEM-2010). The crystal structures of the powders were investigated by Xray diffractometry (XRD, X'Pert PRO MPD) using Cu Kα radiation (λ = 1.5418 Å). The electrochemical properties of the prepared Li_2TiO_3-$LiCrO_2$ composite powders were tested in a 2032-type coin cell. The cathode powder was prepared from a mixture of 20 mg composite powders and 12 mg TAB (TAB is a mixture of 9.6 mg teflonizedacetylene black and 2.4 mg binder). Lithium metal and a microporous polypropylene film were used as the anode and the separator, respectively. The electrolyte was 1 M $LiPF_6$ in a 1:1 mixture by volume of ethylene carbonate/dimethyl carbonate (EC/DMC). The cells were tested in the 2.5-4.5 V potential range at a constant current density of 15 mA g^{-1}.

3. RESULTS AND DISCUSSION

The morphology of the precursor powders for 0.55 Li_2TiO_3-0.45 $LiCrO_2$ nanocomposite powders is shown in Fig. 1.

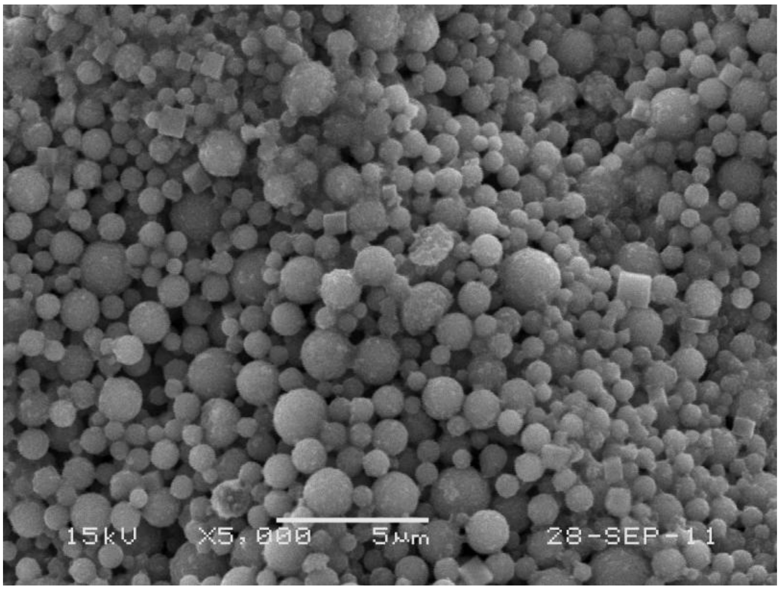

Figure 1. SEM image of the precursor powders prepared by spray pyrolysis.

Because one precursor powder was formed from one droplet by drying, decomposition and crystallization processes inside the hot wall reactor in the spray pyrolysis process, the precursor powders prepared at 1000^{o}C had a spherical shape and micron sizes. However, the precursor powders had an aggregated structure between the powders. The morphologies of the powders prepared by spray pyrolysis are affected by the types of the material because the decomposition and drying characteristics of the precursor salts are different. In particular, lithium and chromium components in the preparation of 0.55 Li_2TiO_3-0.45 $LiCrO_2$ cathode materials by spray pyrolysis in an air atmosphere generate

Li_2CrO_4 glass material with a low melting temperature of 516°C as the impurity phase. Melting of the Li_2CrO_4 glass material resulted in the aggregation between the precursor powders prepared by spray pyrolysis.

To investigate the formation of the 0.55 Li_2TiO_3-0.45 $LiCrO_2$ nanocomposite powders, the precursor powders were post-treated at various temperatures in an air atmosphere and washed with distilled water. The crystal structures and morphologies of the composite powders before and after washing were observed by XRD and SEM.

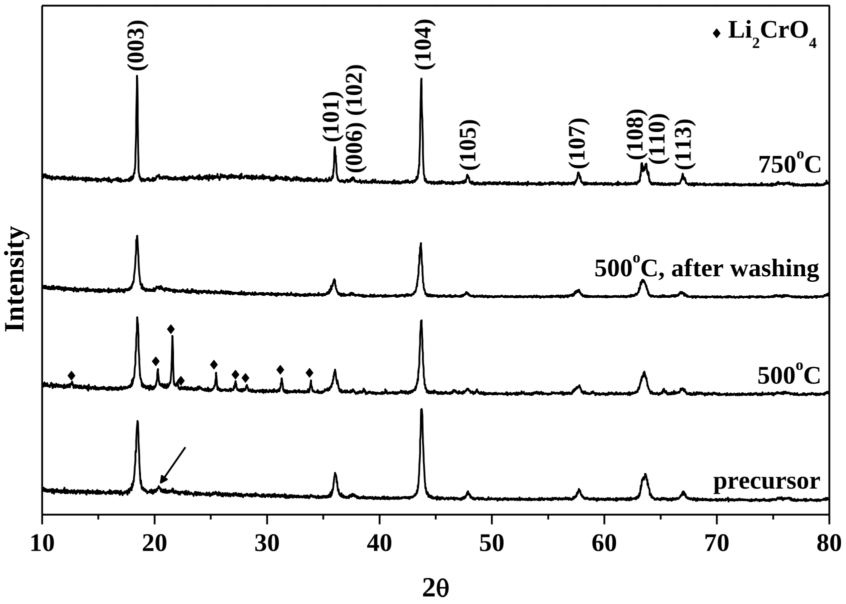

Figure 2. XRD patterns of the precursor and post-treated powders before and after washing.

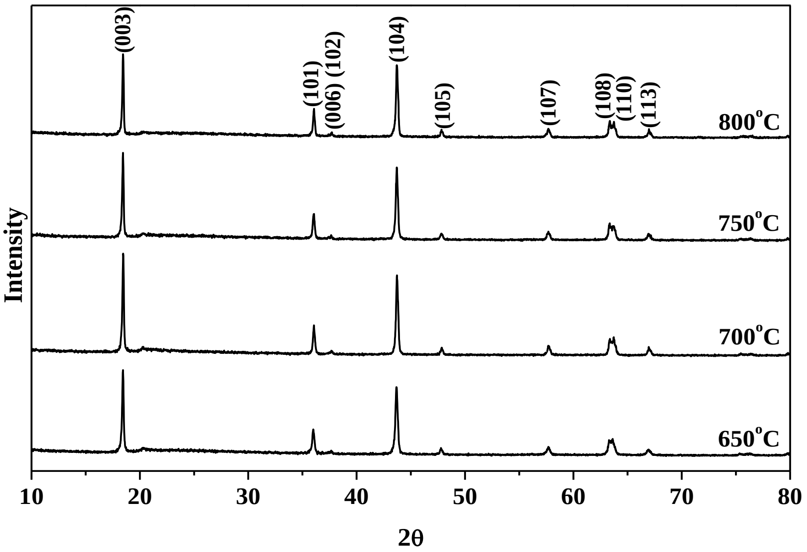

Figure 3. XRD patterns of the powders post-treated at various temperatures after washing.

Figs. 2 and 3 show the XRD patterns of the precursor and post-treated powders. The precursor powders prepared by spray pyrolysis had the mixed crystal structure of the rhombohedral $LiCrO_2$ and the monoclinic Li_2TiO_3 without the impurity phase, in spite of the short residence time of the powders inside the hot wall reactor as 1.7 s. The XRD pattern showed a superlattice peak near 21^o, as indicated by the arrow in Fig. 2, which was due to the short range ordering of the Li, Cr, and Ti in the transition metal layer. The precursor salts of Li, Ti, and Cr components completely decomposed even though there was a short residence time of the powders inside the hot wall reactor. For enough crystal growth, post-treatments of the precursor powders were performed at various temperatures. The XRD pattern of the powders post-treated at a low temperature of 500^oC as shown in Fig. 2 showed the peaks of the Li_2CrO_4 phase. However, the crystal peaks of the Li_2CrO_4 phase were not observed in the XRD pattern of the precursor powders directly obtained by spray pyrolysis. In the precursor powders, Li_2CrO_4 existed in the form of glass material with an amorphous phase because of the high preparation temperature of 1000^oC. Crystallization of Li_2CrO_4 glass material occurred at a post-treatment temperature of 500^oC. The peaks of the Li_2CrO_4 phase in the XRD patterns of the composite powders post-treated at 750^oC as shown in Fig. 2 were not observed. Crystallization of Li_2CrO_4 material did not occur at a higher post-treatment temperature than the melting temperature of Li_2CrO_4. Due to the generation of the impurity Li_2CrO_4 phase in the preparation of the powders at an air atmosphere, washing of the composite cathode powders after post-treatment were required. After washing with distilled water, impurity peaks of the Li_2CrO_4 phase disappeared in the XRD pattern of the powders post-treated at 500^oC.

The composite powders post-treated at various temperatures between 650 and 800^oC were washed with distilled water to eliminate Li_2CrO_4 impurity. Fig. 3 shows the XRD patterns of the washed powders. The washed powders had the mixed crystal structure of the rhombohedral $LiCrO_2$ and the monoclinic Li_2TiO_3 without the impurity phase irrespective of the post-treatment temperatures. The XRD patterns of the composite powders showed a superlattice peak near 21^o irrespective of the post-treatment temperatures.

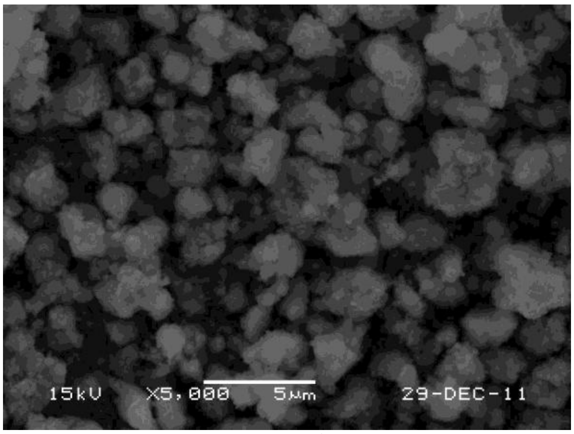

(a) 650^oC

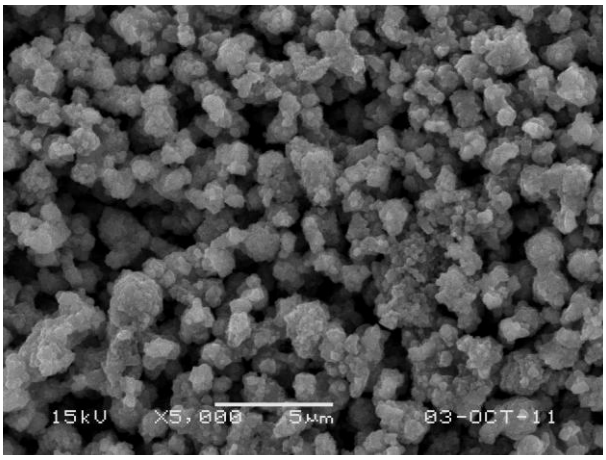

(b) 700°C

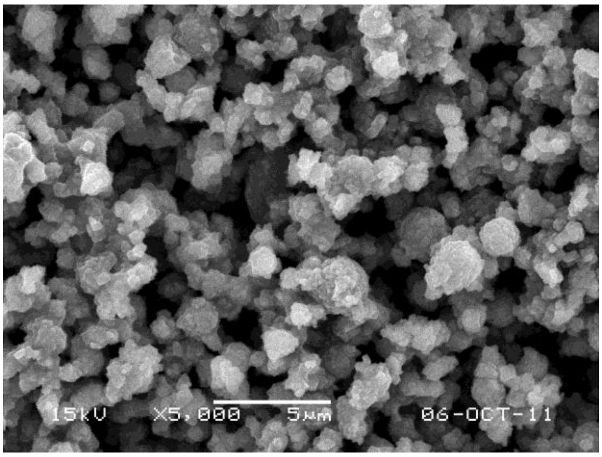

(c) 750°C

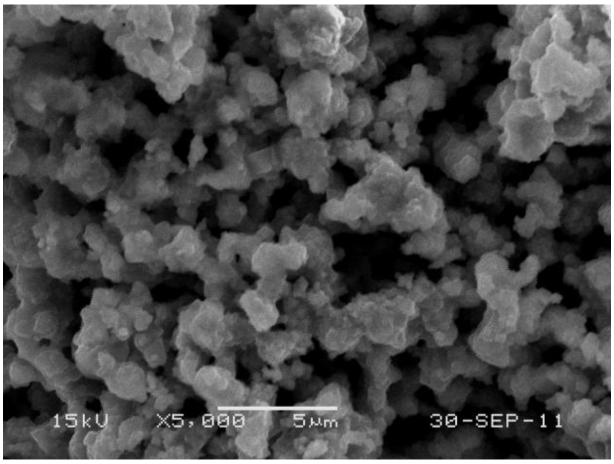

(d) 800°C

Figure 4. SEM images of the powders post-treated at various temperatures before washing.

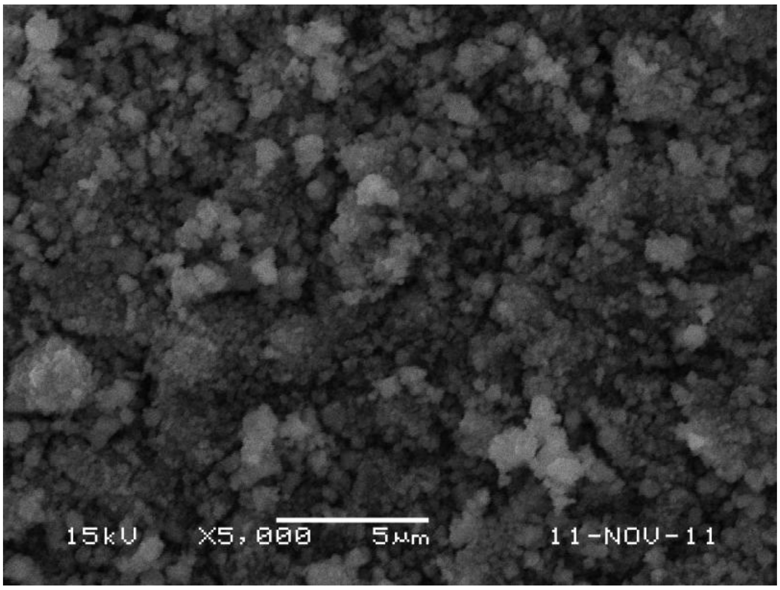

(a) SEM

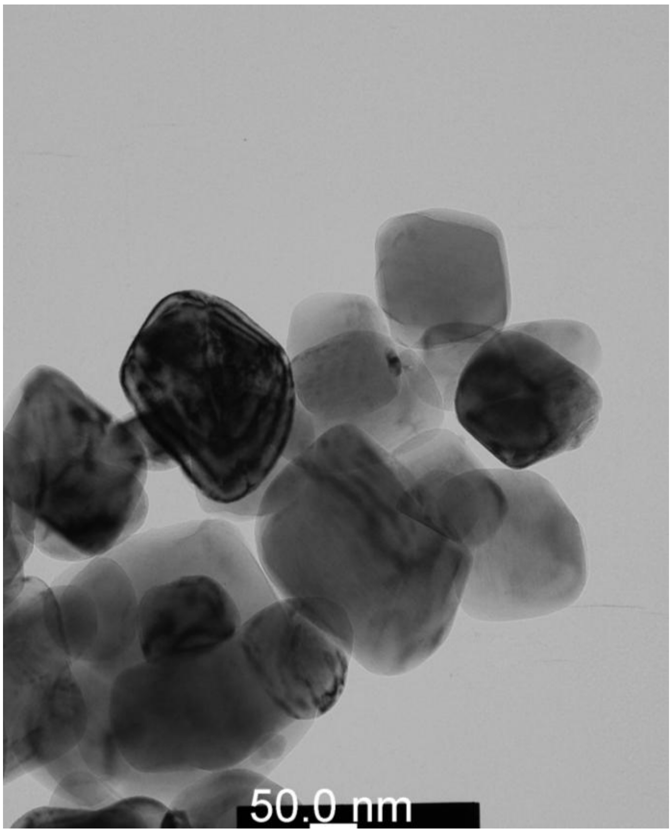

(b) TEM

Figure 5. SEM and TEM images of the powders post-treated at 750^{o}C after washing.

The mean crystallite sizes of the washed powders post-treated at 650, 700, 750, and 800^{o}C calculated by Scherrer's equation were 49, 57, 57, and 67 nm, respectively. The morphologies of the

0.55 Li_2TiO_3-0.45 $LiCrO_2$ nanocomposite powders before washing are shown in Fig. 4. The precursor powders with a spherical shape and micron sizes turned to the aggregated powders with irregular morphologies after post-treatment. Melting of Li_2CrO_4 glass material transferred the spherical shape of the precursor powders to the aggregated morphologies during the post-treatment process at high temperatures.

Fig. 5 shows the SEM and TEM images of the washed 0.55 Li_2TiO_3-0.45 $LiCrO_2$ nanocomposite powders post-treated at 750°C. After washing, the aggregated nanocomposite powders converted to several hundred nanometer-sized cathode powders without a milling process. The mean size of the nanocomposite powders measured from the TEM image was 130 nm.

To confirm the effect of Li_2CrO_4 glass material on the morphology of the Li_2TiO_3-$LiCrO_2$ nanocomposite powders during the post-treatment process, the precursor powders obtained by spray pyrolysis were washed before post-treatment and then post-treated at 750°C. The morphology of the post-treated powders which were washed before post-treatment was investigated by SEM, as shown in Fig. 6.

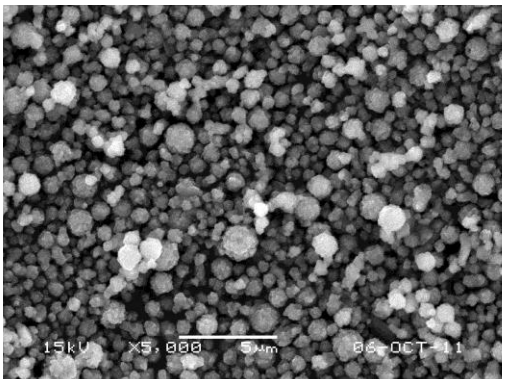

Figure 6. SEM image of the post-treated powders which washing before post-treatment.

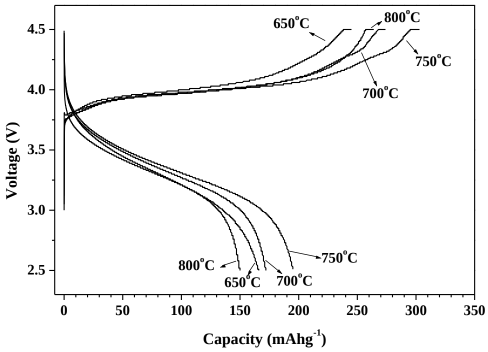

Figure 7. Initial charge/discharge curves of the post-treated powders prepared by spray pyrolysis.

The 0.55 Li_2TiO_3-0.45 $LiCrO_2$ nanocomposite powders still maintained the spherical shape of the precursor powders even after post-treatment. In addition, the washing process of the post-treated powders did not change the spherical morphology of the post-treated Li_2TiO_3-$LiCrO_2$ powders. Therefore, the existence of Li_2CrO_4 glass material during the post-treatment was essential to prepare the aggregation-free 0.55 Li_2TiO_3-0.45 $LiCrO_2$ nanocomposite powders.

The electrochemical properties of the washed 0.55 Li_2TiO_3-0.45 $LiCrO_2$ nanocomposite cathode samples were investigated in the voltage range of 2.5-4.5 V at a constant current density of 15 mA g^{-1}. Initial charge/discharge curves of the 0.55 Li_2TiO_3-0.45 $LiCrO_2$ nanocomposite samples are shown in Fig. 7. All samples show a similar shape of charge/discharge curves irrespective of the post-treatment temperatures. The initial charge capacities of the cathode samples were 245, 274, 303, and 264 mAh g^{-1} when the post-treatment temperatures of the powders were 650, 700, 750, and 800°C, and the Coulombic efficiencies of the first cycles of the cells were 68, 63, 64, and 57 %, respectively. The irreversible capacities of the cathode samples post-treated at 650, 700, 750, and 800°C were 79, 102, 108, and 114 mAh g^{-1}, respectively. The high first-cycle irreversible capacity loss of the cell is similar to that of the 0.55 Li_2TiO_3-0.45 $LiCrO_2$ composite powders prepared by liquid solution methods [18,24]. The 0.55 Li_2TiO_3-0.45 $LiCrO_2$ nanocomposite powders post-treated at 750°C had the highest initial charge and discharge capacities.

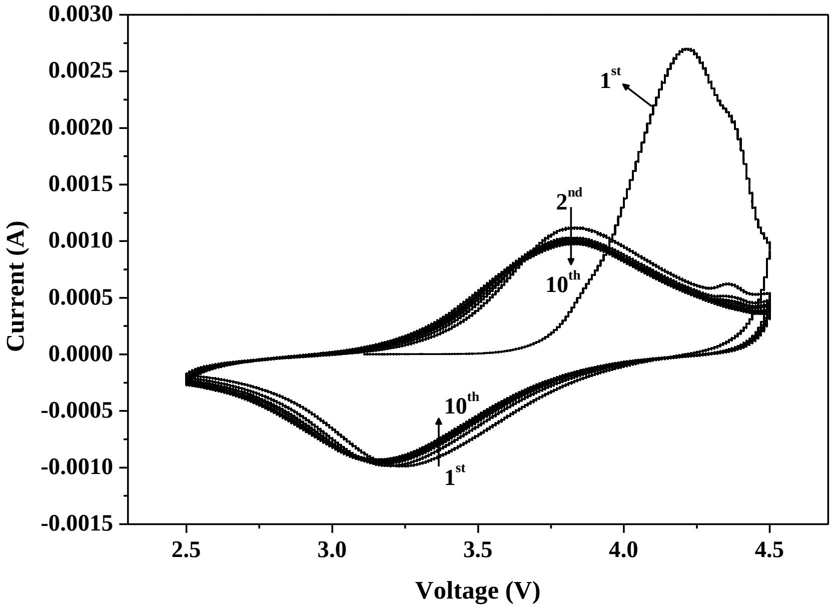

Figure 8. Cyclic voltammogram of the washed sample after post-treatment at 750°C.

Fig. 8 shows the cyclic voltammograms of the 0.55 Li_2TiO_3-0.45 $LiCrO_2$ nanocomposite powders post-treated at 750°C at a scan rate of 0.07 mV s^{-1}. There was a critical difference between the first cycle and subsequent cycles. During cycling, three electrons of the Cr ions are oxidized and reduced, and moved in and out of the transition metal/lithium layer. At the first cycle, partial Cr^{3+} irreversibly moves to the octahedral site in the lithium layer, and this process causes the high irreversible capacity loss as shown in Fig. 7 [18,24]. The peaks positions of the cyclic voltammograms did not change during the subsequent cycles, and this result indicates that the 0.55 Li_2TiO_3-0.45 $LiCrO_2$ nanocomposite powders prepared by spray pyrolysis have good cycle stability.

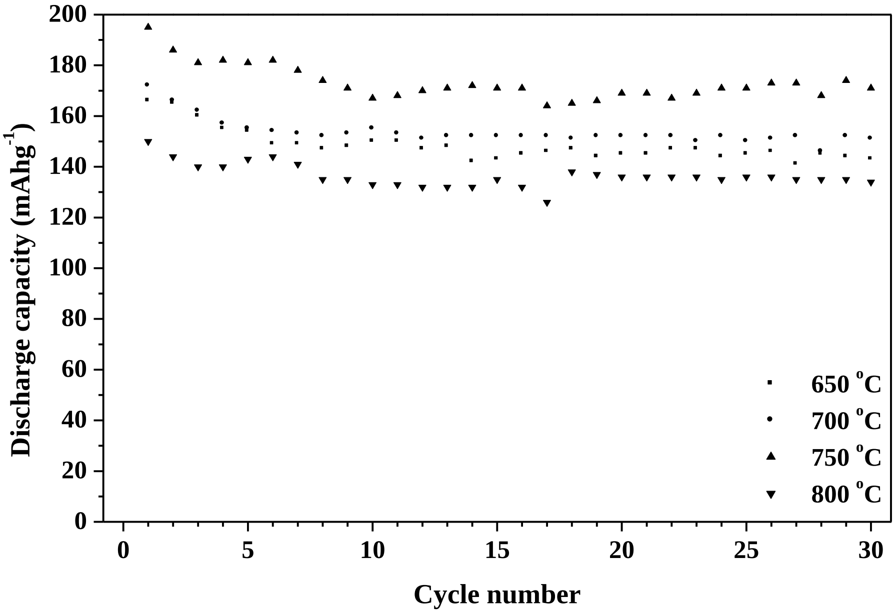

Figure 9. Cycle properties of the powders post-treated at various temperatures.

Cycle properties of the 0.55 Li_2TiO_3-0.45 $LiCrO_2$ nanocomposite samples post-treated at various temperatures are shown in Fig. 9. After 30 cycles, the discharge capacities of the 0.55 Li_2TiO_3-0.45 $LiCrO_2$ nanocomposite samples post-treated at 650, 700, 750, and 800°C decreased from 166, 172, 195, and 150 mAh g^{-1} to 143, 151, 171, and 134 mAh g^{-1}, respectively. The capacity retentions of the cathode powders post-treated at 650, 700, 750, and 800°C were 86, 88, 88, and 89 %, respectively.

4. CONCLUSIONS

The physical and electrochemical properties of the 0.55 Li_2TiO_3-0.45 $LiCrO_2$ nanocomposite powders prepared by spray pyrolysis were investigated. Li_2CrO_4 glass material was formed by an impurity phase in the preparation process of the composite powders. The glass material enabled the formation of the nanometer-sized 0.55 Li_2TiO_3-0.45 $LiCrO_2$ nanocomposite powders. After washing the Li_2CrO_4 glass material with distilled water, the post-treated powders converted to several hundred nanometer-sized composite cathode powders without a milling process. The 0.55 Li_2TiO_3-0.45 $LiCrO_2$ nanocomposite powders post-treated at 750^oC had the highest initial charge and discharge capacities. The results of cyclic voltammograms indicated that the 0.55 Li_2TiO_3-0.45 $LiCrO_2$ nanocomposite powders prepared by spray pyrolysis have good cycle stability.

References

1. R.J. Cummow, D.C. Liles, M.M. Thackeray, *Mater. Res. Bull*., 28 (1993) 1249.
2. G. Vitins, K. West, *J. Electrochem. Soc*., 144 (1997) 2587.
3. J. Wang, Y. Xia, X. Yao, M. Zhang, Y. Zhang, Z. Liu, *Int. J. Electrochem. Sci*., 6 (2011) 6670.
4. C. Deng, Y.H. Sun, S. Zhang, Y. Shang, Z. Dong, Y.X. Wu, *Int. J. Electrochem. Sci*., 7 (2012) 10047.
5. S.S. Shin, Y.K. Sun, K. Amine, *J. Power Sources*, 112 (2002) 634.
6. X. Lu, Z. Chen, J.R. Dahn, *Chem. Mater.*, 15 (2003) 3214.
7. M. Tabuchi, K. Tatsumi, S. Morimoto, S. Nasu, T. Saito. Y. Ikeda, *J. Appl. Apps*., 104 (2008) 043909.
8. Y. Sun, Y. Shiosaki, Y. Xia, H. Noguchi, *J. Power Sources,* 159 (2006) 1353.
9. J.H. Kim, Y.K. Sun, *J. Power Sources*, 119-121 (2003) 166.
10. D. Kim, J. Gim, J. Lim, S. Park, J. Kim, *Mater. Res. Bull*., 45 (2010) 252.
11. M.M. Thackeray, S.H. Kang, C.S. Johnson, J.T. Vaughey, R. Benedek, S.A. Hackney, *J. Mater. Chem*., 17 (2007) 3112.
12. B. Ammundsen, J. Paulsen, *Adv. Mater*., 13 (2001) 943.
13. M.M. Thackeray, C.S. Johnson, J.T. Vaughey, N. Li, S.A. Hackney, *J. Mater. Chem*., 15 (2005) 2257.
14. C.W. Park, S.H. Kim, K.S. Nahm, H.T. Chung, Y.S. Lee, J.H. Lee, S. Boo, J. Kim, *J. Alloys Compd*., 449 (2008) 343.
15. Z. Lu, J.R. Dahn, *J. Electrochem.Soc*., 149 (2002) A1454.
16. X. Wu, S.H. Chang, Y.J. Park, K.S. Ryu, *J. Power Sources*, 137 (2004) 105.
17. B. Ammundsen, J. Paulsen, I. Davidson, R.S. Liu, C.H. Shen, J.M. Chen, L.Y. Jang, J.F. Lee, *J. Electrochem. Soc*., 149 (2002) A431.
18. M. Balasubramanian, J. McBreen, I.J. Davidson, P.S. Whitfield, I. Kargina, *J. Electrochem. Soc.*, 149 (2002) A176.
19. J.S. Kim, C.S. Johnson, M.M. Thackeray, *Electrochem. Commun*., 4 (2002) 205.
20. C.S. Johnson, J.S. Kim, A.J. Kropf, A.J. Kahaian, J.T. Vaughey, M.M. Thackeray, *J. Power Sources*, 119-121 (2003) 139.
21. J.S. Kim, C.S. Johnson, J.T. Vaughey, M.M. Thackeray, S.A. Hackney, W. Yoon, C.P. Grey, *Chem. Mater*., 16 (2004) 1996.
22. L. Zhang, H. Noguchi, *J. Electrochem. Soc*., 150 (2003) A601.
23. L. Zhang, H. Noguchi, *Electrochem. Commun*., 4 (2002) 560.
24. X. Mi, H. Li, X. Huang, *J. Power Sources*, 174 (2007) 867.
25. S.H. Park, C.S. Yoon, S.G. Kang, H.S. Kim, S.I. Moon, Y.K. Sun, *Electrochim. Acta*, 49(2004) 557.
26. I. Taniguchi, D. Song, M. Wakihara, *J. Power Sources*, 109 (2002) 333.
27. Y.N. Ko, H.Y. Koo, J.H. Kim, J.H. Yi, Y.C. Kang, J.H. Lee, *J. Power Sources*, 196 (2011) 6682.
28. S.H. Choi, J.H. Kim, Y.N. Ko, Y.J. Hong, Y.C. Kang, *J. Power Sources*, 210 (2012) 110.